

# METAL-POOR STARS ON DISC-LIKE ORBITS: INSIGHTS FROM PRISTINE-GAIA SYNTHETIC

I. González Rivera de La Vernhe<sup>1</sup>, V. Hill<sup>1</sup>, G. Kordopatis<sup>1</sup>, F. Gran<sup>1</sup>, E. Fernández-Alvar<sup>2</sup> and the Pristine collaboration

**Abstract.** Metal-poor stars provide invaluable information about the onset of the Milky Way’s main components, especially through the investigation of their chemodynamics. Recently, a number of studies uncovered a population of metal-poor stars with orbital properties classically associated with the Galactic disc (prograde and planar motion), together with high angular momenta and high rotational velocities. We combined photometric metallicities from the Pristine-*Gaia* catalogue with *Gaia* astrometry to construct a robust sample of giant stars with chemodynamical information down to the lowest metallicities, in order to investigate this peculiar population. Although the majority of our sample matches the orbital characteristics of the Galactic halo, we confirmed the presence of a very metal-poor disc-like subset of stars, which given the evidence drawn from several kinematic spaces, seems to belong to a metal-weak thick disc component.

Keywords: Galaxy: disc , Galaxy: kinematics and dynamics , Galaxy: formation , Catalogues , Surveys

## 1 Introduction

Metal-poor stars are essential to constrain the early history of the Milky Way, as they are believed to be some of the oldest objects in the Universe. When combining their chemical and orbital properties, metal-poor stars retain key information about the primordial onset of the Galactic components. In particular, the origin and formation of the Galactic disc have been and still are highly debated. Although the  $\lambda$ CDM formation scenario predicts that the most metal-poor stars should reside on pressure-supported orbits (in the bulge or the halo, e.g. Starkenburg et al. 2017b), recent studies unveiled the presence of metal-poor ( $[\text{Fe}/\text{H}] < -1.0$ ) stars on disc-like orbits, namely with high rotational velocities, low eccentricities, and low maximum scale heights (Sestito et al. 2019, 2020; Venn et al. 2020; Fernández-Alvar et al. 2021; Viswanathan et al. 2024; Nepal et al. 2024).

Within the last 30 years, consequential progress has been made in the detection of metal-poor stars through the development of ground and space-based spectroscopic and photometric surveys. Among them, the Pristine survey (Starkenburg et al. 2017a) was specifically designed to target the most metal-poor stars of the Galaxy. The photometric survey, based at the Canada-France-Hawaii Telescope (CFHT) at the Mauna Kea Observatory in Hawaii, uses a narrow-band metallicity-sensitive filter centered on the Ca H & K doublet lines, with the aim of providing metallicity estimates for the metal-poor candidates of Galaxy. So far, Pristine has been able to map more than  $6500 \text{ deg}^2$  of the northern sky and has uncovered a large number of very, extremely, and ultra metal-poor stars. As part of the first data release of the Pristine survey, Martin et al. (2023) published the Pristine-*Gaia* synthetic (PGS) catalogue, which contains 52 million photometric metallicities derived from *Gaia* BP/RP spectro-photometry. Thanks to its full sky coverage and bright targets ( $G < 16 \text{ mag}$ ), we can get a clearer chemodynamical picture of the early days of each Galactic component.

In this work, we aim to characterise the underlying disc-like metal-poor population found in Fernández-Alvar et al. (2021) and several recent works. We combined reliable photometric estimates from the PGS metallicity catalogue with astrometric parameters from the third data release of the *Gaia* mission to create a statistically robust sample of  $\sim 36\,000$  very metal-poor (VMP) giant stars ( $[\text{Fe}/\text{H}] < -1.7$ ). We refined the catalogue by discarding spurious photometric metallicity estimates, using spectroscopic surveys such as APOGEE, GALAH, LAMOST, and *Gaia* RVS GSP-spec.

<sup>1</sup> Université Côte d’Azur, Observatoire de la Côte d’Azur, CNRS, Laboratoire Lagrange, 06304 Nice, France

<sup>2</sup> Instituto de Astrofísica de Canarias, Departamento de Astrofísica, Universidad de La Laguna, E-38200 La Laguna, Tenerife, Spain

## 2 Constructing a robust sample of metal-poor stars with *Gaia* RVS and Pristine-*Gaia* synthetic

To investigate the disc-like metal-poor candidates, it is very important to develop a robust method that only selects genuine metal-poor stars. We expect the distribution of the thin disc to be essentially metal-rich (Hayden et al. 2015; Kordopatis et al. 2015), therefore finding a large number of metal-poor stars with disc features is surprising. To avoid having a small fraction of metal-rich disc stars compromising the detection of a kinematically cold metal-poor population, we implemented several steps in our method. First, we applied a number of *Gaia* astrometry and PGS quality cuts, as well as stellar population cuts (e.g. discarding stellar and globular cluster members); in particular, following Fernández-Alvar et al. (2021), we restricted our study to giant stars only. A detailed description of the cuts is provided in Sec. 3 of González Rivera de La Vernhe et al. (2024). We then developed an isochrone filtering method dedicated to capturing genuine metal-poor stars in the colour-magnitude diagram (CMD), using arguments of age and metallicity to justify the physicality of their location. Altogether, we were able to construct a sample of  $\sim 3\text{M}$  giant stars, including  $\sim 54\,000$  metal-poor stars ( $[\text{Fe}/\text{H}] < -1.5$  dex) with reliable photometric metallicities from PGS and orbital parameters from *Gaia* RVS GSP-spec. Details on the computation of the orbital parameters are given in Sec. 2 of González Rivera de La Vernhe et al. (2024). The method was validated using the spectroscopic metallicity catalogues of APOGEE DR17, GALAH DR3, LAMOST DR8, and GSP-spec as detailed in Sec. 4.1 of González Rivera de La Vernhe et al. (2024). We then used the corresponding spectroscopic contaminants to statistically decontaminate our sample of PGS stars below  $-1.7$  dex ( $\sim 36\,000$  stars).

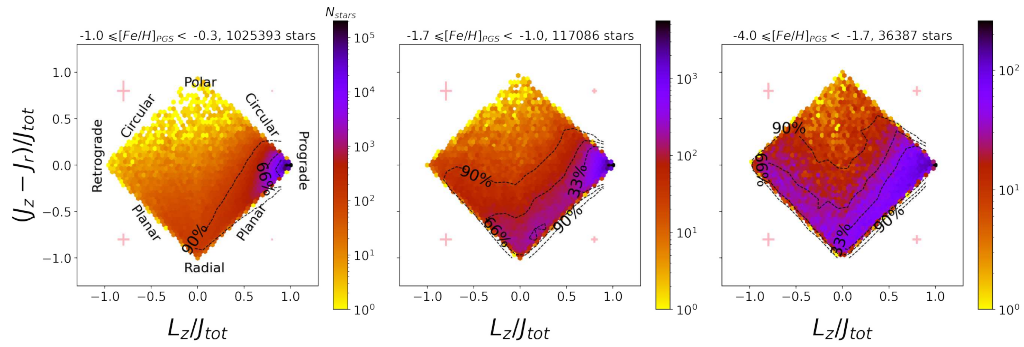


**Fig. 1.** Action space:  $(J_z - J_r)$  as a function of  $L_z$ . Axes are normalised by  $J_{tot} = |L_z| + J_r + J_z$ . **Left:**  $-1.0 < [\text{Fe}/\text{H}]_{\text{PGS}} < -0.3$ . **Middle:**  $-1.7 < [\text{Fe}/\text{H}]_{\text{PGS}} < -1.0$ . **Right:**  $-4.0 < [\text{Fe}/\text{H}]_{\text{PGS}} < -1.7$ . We note that the colour bar range changes for each interval. We add mean error bars for each quadrant of the action space in light pink.

The action space of the filtered PGS is displayed in Fig. 1. We used this space to properly identify different families of orbits, tracing the main Galactic components. In the left panel, associated with the most metal-rich interval ( $-1.0 < [\text{Fe}/\text{H}] < -0.3$ ), we observe a majority of prograde-planar-circular stars, in agreement with a thin disc population. As we explore lower metallicity intervals, we expect to find significantly fewer stars in the disc-like area of the action space, and a majority of stars on retrograde orbits, more characteristic of the halo. However, as seen in the middle panel, while the overall 90% of the sample is shifted towards retrograde orbits, we notice a strong prograde-retrograde asymmetry, in favour of prograde stars. This asymmetry is also visible down to the lowest metallicity regime, below  $-1.7$  dex. Through the statistical decontamination in the  $V_\phi - [\text{Fe}/\text{H}]$  and in the action space described in Sec. 5 of González Rivera de La Vernhe et al. (2024), we confirmed that the metal-poor disc-like population of PGS could not be eliminated, and actually represented a high fraction of stars. Such findings called for an in-depth investigation of the highly prograde ( $V_\phi > 180 \text{ km s}^{-1}$ ), planar, and very metal-poor ( $[\text{Fe}/\text{H}] < -1.7$  dex) PGS subset, in order to provide a more complete kinematical and dynamical characterisation.

## 3 Characterising the metal-poor disc-like population

### 3.1 The $Z_{\text{max}} - R_{\text{max}}$ distribution

Following Haywood et al. (2018), we investigated the  $Z_{\text{max}} - R_{\text{max}}$  plane, of interest to constrain the bulk of distribution of each Galactic component. We compared our PGS sample with the Gaia Universe Model Snapshot

(GUMS, Robin et al. 2012), which provides a first estimate of the theoretical distribution of the Galactic thin disc, thick disc and halo. The parameters chosen for the Galactic components are constrained by the Besançon Galaxy Model\* (BGM, Robin et al. 2003). To achieve a proper comparison, we selected the GUMS nearest neighbour of each PGS star in latitude  $\ell$ , longitude  $b$ , parallax  $\varpi$ , and apparent G magnitude. The resulting plot is shown in Fig. 2. Each panel shows the distribution of a single GUMS Galactic component (from left to right: thin disc, thick disc, halo), with the 66% contour line of the distribution in red. We overplot the 66% contour line of our PGS VMP comparison sample in yellow. Solid lines correspond to the entire sample while dashed lines only show the highly prograde PGS VMP subset ( $V_\phi > 180 \text{ km s}^{-1}$ ). Overall, we find that the GUMS thin disc (left panel of Fig. 2) is essentially located towards the Galactic plane (i.e. 84 % of the distribution below  $Z_{\text{max}} = 2 \text{ kpc}$ ), which greatly differs from the distribution of our PGS sample (only 22 % when considering the full PGS VMP sample). Therefore, we can exclude that the PGS VMP highly prograde population originates from a thin disc component. Regarding the GUMS thick disc and halo (middle and right panels), the similarities with PGS are less evident, which is why we focused on the fraction of stars below  $Z_{\text{max}} = 2 \text{ kpc}$ . We find that the best match in fraction for the full PGS VMP sample is the GUMS halo; however, the PGS VMP highly prograde subset finds its best match in the GUMS thick disc. The R-Z spatial distribution of that same subset (see Sec. 6.1.1 of González Rivera de La Vernhe et al. 2024) is also compatible with a short-scaled thick disc, a hint that the VMP highly prograde population could originate from a thick disc component.

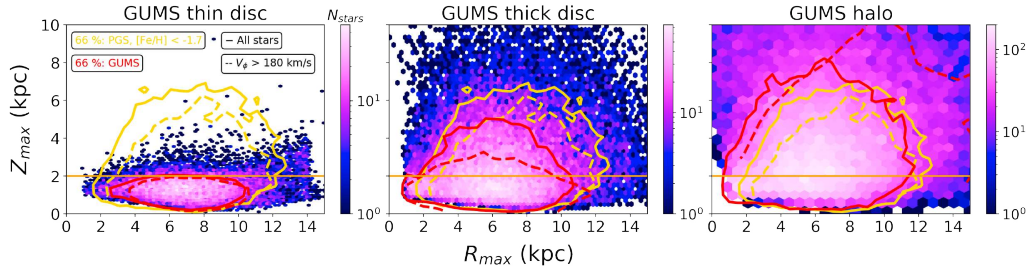


**Fig. 2.**  $Z_{\text{max}}$  as a function of  $R_{\text{max}}$ . The density plot corresponds to GUMS stars that follow the selection function of the PGS VMP sample (below  $[\text{Fe}/\text{H}] = -1.7$ ) in  $\ell$ ,  $b$ ,  $\varpi$ , and apparent G magnitude. The red solid line corresponds to the 66 % contour line of each GUMS sample, while the yellow solid line is the 66 % contour line of PGS VMP stars ( $[\text{Fe}/\text{H}] < -1.7$ ). The red dashed line corresponds to the 66 % contour line of each highly prograde ( $V_\phi > 180 \text{ km s}^{-1}$ ) GUMS subsample; the yellow dashed line is the 66 % contour line of PGS VMP highly prograde stars. The orange solid horizontal line corresponds to  $Z_{\text{max}} = 2 \text{ kpc}$ . **Left:** GUMS thin disc. **Middle:** GUMS thick disc. **Right:** GUMS halo.

### 3.2 Asymmetries in the $V_\phi$ distribution and in the action space

To understand to what extent the Galactic halo contributes to the PGS VMP subset, we tried to remove the kinematic signature of a halo, in the  $V_\phi$  distribution and in the action space, from the PGS VMP subset. We assumed that the halo is centered at  $V_\phi = 0 \text{ km s}^{-1}$ , corresponding to a zero net rotation. In both kinematic spaces, we progressively subtracted the retrograde (halo-like) component of the PGS distribution from the prograde (disc-like) component and checked at which  $V_\phi$  value or action space area lies the remainder of counts. A minimum of counts in highly prograde areas ( $> 200 \text{ km s}^{-1}$ ) means that we cannot observe the signature of a highly prograde metal-poor substructure; therefore our population of interest would solely be contributed by the halo. This approach, although not free of hypothesis, is free of assumptions regarding the modelling and form of the velocity distributions. In the  $V_\phi$  space, we find that  $40 \text{ km s}^{-1}$  is the value that globally minimises the prograde VMP population. Therefore, the population could be considered as the high-rotation tail of a prograde halo centered at this value, in agreement with the results of Zhang et al. (2023), who fitted three-dimensional Gaussian Mixture Models using a sample of stars with Gaia RVs and metallicities from Andrae et al. (2023). However, as seen in the right panel of Fig. 3, we find that stars with prograde-planar and circular orbits remain

\*[https://gea.esac.esa.int/archive/documentation/GEDR3/Data\\_processing/chap\\_simulated/sec\\_cu2UM/ssec\\_cu2starsgal.html](https://gea.esac.esa.int/archive/documentation/GEDR3/Data_processing/chap_simulated/sec_cu2UM/ssec_cu2starsgal.html)

after subtracting the retrograde subset of the PGS VMP population. This result suggests that the PGS VMP highly prograde and planar population cannot solely be contributed by a canonical halo.

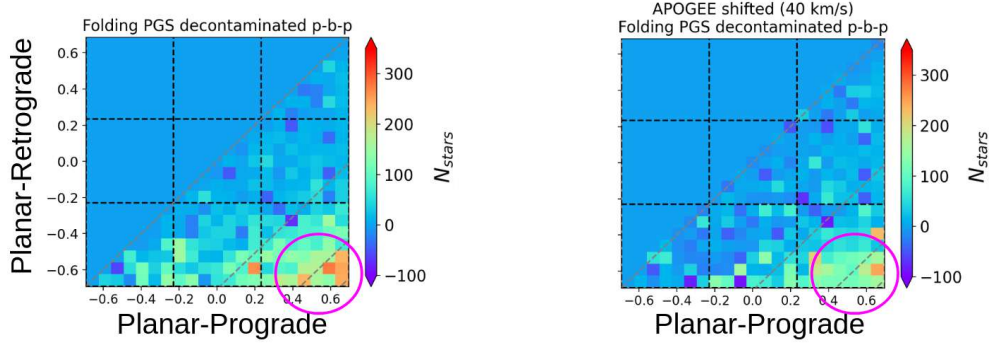


**Fig. 3.** Rotated action space between  $-4.0 < [\text{Fe}/\text{H}] < -1.7$ . The grey dashed lines correspond to different values of  $L_z/J_{\text{tot}}$ :  $[-0.95, -0.8, -0.5, 0, 0.5, 0.8, 0.95]$ . **Left:** folding of the retrograde components over the prograde components, for PGS decontaminated pixel-by-pixel using APOGEE contamination. In this space, the folding axis of symmetry is the grey dashed line at  $L_z/J_{\text{tot}} = 0$ . **Right:** same, but the three actions were computed shifting the observed  $V_\phi$  by  $40 \text{ km s}^{-1}$ .

## 4 Conclusions

We found that, although the global distribution of the PGS sample matches a typical halo in orbital properties and kinematics, there is an evident asymmetry in the distribution of stars, in  $V_\phi$  and  $L_z$ , in favour of prograde stars down to  $\sim -2.9$  dex. Within this subset of VMP prograde stars lies a subgroup with high  $V_\phi$  and low eccentricities, which bears characteristics typical of a thick disc. Several pieces of evidence found in various kinematic spaces lead to believe that this disc-like metal-poor population could be part of a metal-weak thick disc instead of a halo, reminiscent of structures like the Atari disc. Nonetheless, a spectral analysis is needed to determine whether the population was formed in or ex situ. This could clear the different scenarios envisioned for its origin(s), for example whether it migrated onto the disc due to mechanisms involving the Galactic bar or oscillations of halo stars, or whether it is a dwarf galaxy remnant as suggested in recent studies. We believe that elemental abundances are key to reconstructing this chapter of the Galactic disc's history.

## References

- Andrae, R., Rix, H.-W., & Chandra, V. 2023, *ApJS*, 267, 8
- Fernández-Alvar, E., Kordopatis, G., Hill, V., et al. 2021, *MNRAS*, 508, 1509
- González Rivera de La Vernhe, I., Hill, V., Kordopatis, G., et al. 2024, arXiv e-prints, arXiv:2406.05728
- Hayden, M. R., Bovy, J., Holtzman, J. A., et al. 2015, *ApJ*, 808, 132
- Haywood, M., Di Matteo, P., Lehnert, M. D., et al. 2018, *ApJ*, 863, 113
- Kordopatis, G., Wyse, R. F. G., Gilmore, G., et al. 2015, *A&A*, 582, A122
- Martin, N. F., Starkenburg, E., Yuan, Z., et al. 2023, submitted to *A&A*, arXiv:2308.01344
- Nepal, S., Chiappini, C., Queiroz, A. B. A., et al. 2024, accepted for publication in *A&A*, arXiv:2402.00561
- Robin, A. C., Luri, X., Reylé, C., et al. 2012, *A&A*, 543, A100
- Robin, A. C., Reylé, C., Derrière, S., & Picaud, S. 2003, *A&A*, 409, 523
- Sestito, F., Longeard, N., Martin, N. F., et al. 2019, *MNRAS*, 484, 2166
- Sestito, F., Martin, N. F., Starkenburg, E., et al. 2020, *MNRAS*, 497, L7
- Starkenburg, E., Martin, N., Youakim, K., et al. 2017a, *MNRAS*, 471, 2587
- Starkenburg, E., Oman, K. A., Navarro, J. F., et al. 2017b, *MNRAS*, 465, 2212
- Venn, K. A., KIELTY, C. L., Sestito, F., et al. 2020, *MNRAS*, 492, 3241
- Viswanathan, A., Yuan, Z., Ardern-Arentsen, A., et al. 2024, submitted to *A&A*, arXiv:2405.13124
- Zhang, H., Ardern-Arentsen, A., & Belokurov, V. 2023, submitted to *MNRAS*, arXiv:2311.09294